ON THE PHYSICAL MECHANISMS FOR THE NUMERICAL MODELLING OF FLOWS AROUND AIR LUBRICATED SHIPS

G. Rotte[1], O. Zverkhovskyi[2], M. Kerkvliet[3] and T. van Terwisga[1,3]
[1]Dept. of Ship Hydromechanics and Structures, Delft University of Technology
Mekelweg 2, 2628 CD Delft, The Netherlands
[2]Damen Shipyards Gorinchem
Avelingen West 20, 4202 MS Gorinchem, the Netherlands
[3]Maritime Research Institute Netherlands,
Haagsteeg 2,6708 PM Wageningen, The Netherlands
G.M.Rotte@tudelft.nl, sasha.zverkhovskyi@damen.com, M.Kerkvliet@marin.nl,
T.v.Terwisga@marin.nl

ABSTRACT: Air lubrication techniques are very promising in reducing ship drag. It has been demonstrated that air cavity applications can realise propulsive power reduction percentages of 10-20% due to the reduction of the frictional resistance [1, 2]. However, a complete understanding of the two-phase flow physics involved with air cavity flows is still missing. Multiphase CFD methods can help to get a better understanding of these physics. The largest challenge in predicting the air cavity characteristics lies in the correct modelling of their closure (reattachment) region [3, 4]. In this region the separated air-water flow transforms into a more dispersed flow. The transformation is partly caused by instabilities in the two-phase flow. This article aims to link the physical modelling of the relevant phenomena to their numerical modelling. The link to the numerical modelling is addressed with an emphasis on different RaNS and hybrid RaNS-LES turbulence models. The article is based on the available literature in the public domain and knowledge gained in research projects carried out at Delft University of Technology and Maritime Research Institute Netherlands (MARIN).

INTRODUCTION

The international shipping industry is responsible for a significant part of the world's air pollution. Air lubrication techniques have realised total propulsive power reduction percentages of 10-20% [1, 2] and could possibly realise pollution reduction percentages in the same order of magnitude. However, the physics involved with these flows are not yet completely understood, holding back the application of air lubrication techniques in practical ship design.

Flows around air lubricated ships can be described by two flow regimes where air is distributed in water: the stratified and the dispersed regime (Figure 1). The stratified regime is characterised by a sustained gas layer between the body surface and the liquid, whereas the dispersed regime is characterised by the liquid around the body being saturated with gas bubbles. The main focus in this article is on the stratified regime. This is the most attractive flow regime when aiming for frictional drag reduction since the local wall friction of a submersed body is mainly prescribed by the viscosity, density and the velocity gradient in the boundary layer [2].

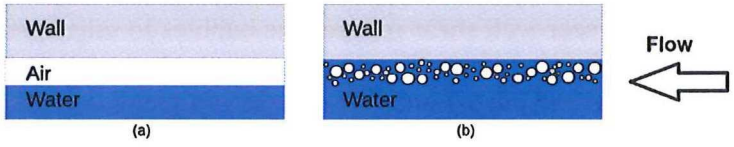

Figure 1 – Air lubrication techniques: stratified regime (a) and dispersed regime (b)

To understand the multiphase flow physics involved as well as to lower the threshold for the application of these techniques, the behaviour of these flows is to be modelled numerically. The main goal of the current research is to gain the required knowledge and understanding to accurately predict the pressure- and shear stress distributions along a ship hull equipped with an air lubrication system using multiphase CFD. As found by Zverkhovskyi et al.[3] and Shiri et al.[4] the key to the numerical prediction of the air layer characteristics lies in the correct modelling of the closure region, where the stratified flow transforms into a more dispersed/bubbly flow. The relevant mechanisms causing this transition are identified in this article, enabling one to identify the CFD method which is capable of modelling these flows.

1. CLASSIFICATION OF AIR LUBRICATION METHODS

Several research groups investigated air lubrication techniques. In this process, different authors used different names for similar techniques, or similar names for different techniques. This section will summarise the different physical mechanisms behind the available air lubrication techniques. They all aim to reduce the ship's frictional drag, which is mainly prescribed by the viscosity, density and the velocity gradient in the boundary layer. The flow regimes of interest for typical cargo ships at full scale are characterised by relatively low Froude ($O(0.2)$) and high Reynolds numbers ($O(10^9)$) (Eqs. 1 and 2 respectively). Here $\mathbf{V}$ is the ship speed, $\mathbf{g}$ is the gravitational constant, $\mathbf{L}$ is the ship length and ν is the kinematic viscosity of water.

$$\mathbf{Fr} = \frac{\mathbf{V}}{\sqrt{\mathbf{gL}}} \tag{1}$$

$$\mathbf{Re} = \frac{\mathbf{VL}}{\nu} \tag{2}$$

1.1 Bubble drag reduction

Bubble drag reduction techniques are here defined as flows in the dispersed regime, where the water is mixed with air bubbles (Figure 1b). Although the dispersed flow regime is not the focus of this current research, it is noted that there is currently a discussion ongoing with respect to the working mechanisms of bubble drag reduction techniques. The most straightforward drag reduction mechanisms are based on a change in the the local mixture density and viscosity (since the difference in density and viscosity between water and air is in the order of 10^3). In both of these cases it is essential that the bubbles remain in the ship's boundary layer (BL) in order to be effective. Murai [5] recently published an extensive review on frictional drag reduction by bubble injection. He classifies different drag reduction mechanisms using the different bubble sizes in the flow. Apart from the above described mechanisms for frictional drag reduction, a change in the BL profile and thus local velocity gradient is described. The exact physical mechanism behind this change in velocity gradient is not fully understood yet. Murai [5] ascribes it to the interaction of the (micro)bubbles with the turbulence structures in the BL. Sanders et al.[6] however report that the frictional drag reduction effect is lost after the first few metres downstream of the air injector in their experiments. They ascribe this effect to bubble-migration: the near-wall shear induces the bubbles to migrate from the wall surface. This finding is confirmed by Harleman [7], who found no evidence of a change in the BL profile. Work by Van den Berg et al.[8] in a Taylor-Couette set-up seems to indicate effectiveness, but herein the gravitational force is different and the flow is confined between two walls.

1.2 Air layer drag reduction

The stratified regime is entered when the liquid phase is completely replaced by the gas phase within the boundary layer. The resulting friction force is in the order of 10^3 times smaller when compared to the friction force of water at the wall due to the difference in density. Within the air layer regime, three different drag reduction techniques are identified: natural air layers, external air cavities and internal air cavities (Figure 2).

Natural air layers (Figure 2a) are formed by supplying a sufficient amount of air to the horizontal wall underneath the ship. When a small 'cavitator' is applied directly upstream of the point of injection, a so-called external cavity can be formed (Figure 2b). The cavitator is creating a suction pressure directly downstream of it, separating the mean flow from the wall. The external cavity needs side fences to remain stable. The third air layer technique is the hull integrated (or simply 'internal') air cavity technique (Figure 2c). Here, a recess is formed in the bottom of the ship hull. This is closed by a beach at the closure. A step-wise stern or backward facing step is separating the mean flow in the upstream region of the target wall.

From a practical point of view, the natural air layer technique requires the highest- and the the internal air cavity the lowest air flux to maintain a stable air layer underneath the ship hull. In comparison to the other two techniques, the natural air layer technique is least stable and most sensitive to misalignment of the surface from the horizontal position [2]. However, it also requires the smallest modification of the ship hull form whereas the internal cavity technique requires the largest modifications. These modifications cause an increase in ship resistance when the air supply system fails or is turned off. This is caused by the added resistance of the recesses/cavitators/fences and the added draft due to the reduction in buoyancy force due to the absence of water underneath the ship hull.

The above mentioned air layer systems will be explained in more detail in sections 1.2.1 through 1.2.3. Here, emphasis is put on the internal- and external cavity techniques, since these are proven to be applicable for ships as reported by Gorbachev and Amromin [1]. Next to the above mentioned air-layer techniques, Ceccio [9] describes both natural and ventilated super-cavity flows, but those cases are not reviewed in this article since they are not applicable for ships.

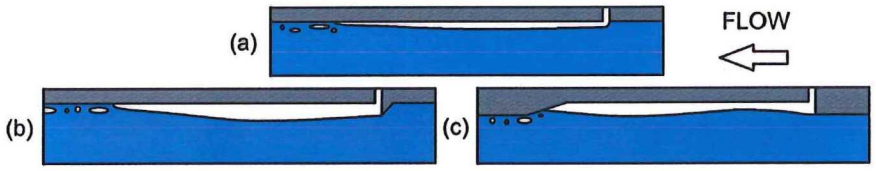

Figure 2 – Air layer techniques:
natural air layer (a), external cavity (b) and hull integrated (internal) cavity (c)

1.2.1 Natural air layers

Natural air layers (Figure 2a) are formed underneath a horizontal surface by injecting a sufficient amount of air trough a (partly) porous wall. Also, a bubbly flow can transform into an air layer flow when a sufficient amount of air is injected [10]. Fukuda [11] reports the use of a super-water-repellent coating that helps to create the air layer underneath the horizontal surface. When the gas layer forms a thin but stable gas film, it is termed the gas film method. Here, both the gas layer and gas film methods are grouped into the gas layer class, while the gas–liquid interface takes different structures in both techniques.

1.2.2 External cavities

The application of the external cavity technique (Figure 2b) results in smaller air losses when compared to the air layer technique. An overview of the work on air cavity ships carried out in the USSR/Russia from 1966 until 2012 is given by Gorbachev and Amromin [1]. A recent study by Zverkhovskyi [2] provided more understanding of the general physics of external air cavities and their drag reduction capability. This study contained flat plate experiments in the TU Delft cavitation tunnel as well as ship model experiments with a number of cavities at the bottom of the ship's hull. The results of that research are briefly summarised here.

Butozov [12] and Matveev [13] have found that the cavity length is equal to approximately a half of the gravity-dominated surface wave length in a steady flow. Zverkhovskyi [2] found that the shallow-water effect can substantially increase the cavity length, and the length and thickness can somewhat be influenced by the initial flow conditions such as the boundary layer thickness as well as by the cavity closure conditions. It was also shown that the angle of attack of the plate has a strong effect on the cavity parameters. This was likely due to the pressure gradient that occurred over the cavity because of the change in cross sectional area of the water tunnel due to the plate inclination. The overall friction on a flat plate can be reduced by up to 60% when external air cavities are applied. This is including the drag penalties due to the wedge (cavitator) and fences at the cavity sides.

For the behaviour in the cavity closure region, two mechanisms governing the air discharge from the cavity were observed. The first mechanism was identified as the re-entrant jet mechanism, continuously shedding bits of air from the cavity. This re-entrant jet behaviour is similar to the shedding behaviour of natural sheet cavities. The second mechanism is governed by waves at the air-water interface. If the wave amplitudes are comparable to the cavity thickness, the cavity breaks up. The contribution of each of these mechanisms depends on the flow conditions (flow velocity, turbulence intensity) and geometry of the cavity. An example of the influence of turbulence intensity on the external cavity surface is given in Figure 3. Two cavities are presented at the same velocity but formed at different longitudinal positions along the plate, meaning different boundary layer thicknesses and thus different turbulence length scales. The cavity at position 4 is less stable compared to the one at position 1. The small scale waves generated by the velocity fluctuations at the interface are much stronger further downstream on the plate. This made the development of a steady cavity with a length equal to a half of the surface wave length impossible.

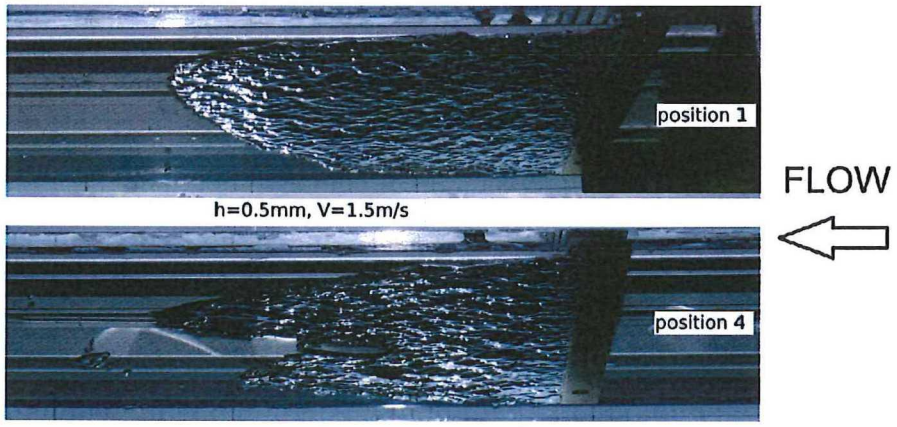

Figure 3 – Cavity stability: Two cavities at the same velocity, formed at different longitudinal positions on the plate. Flow is from right to left (reproduced from[2])

1.2.3 Internal cavities

Hull integrated or internal cavities (Figure 2c) are characterised by the presence of a recess underneath the ship's hull. This concept is also referred to as the air chamber concept. In contrast to the external cavity technique, the free surface is not limited by the wavelength of the gravity-dominated surface wave when the recess is of sufficient depth. A multi-wave cavity can thus be formed.

Shiri et al.[4] have done experimental work on a multi-wave internal cavity system. The cavity profile and stability were investigated at different velocities, air pressure and cavity closure (beach) geometry. The results of these measurements were compared with 2-D and 3-D CFD computations (RaNS/Volume Of Fluid).

Mäkiharju [14] reports experiments on internal air cavities in the U.S. Navy's W. B. Morgan Large Cavitation Tunnel. He reports that the gas flux needed to establish the cavity is higher than the flux needed to maintain the cavity. The required air flux in steady flow is a function of Froude number, Reynolds number, Weber number and closure geometry. In other words, inertial, viscous as well as surface tension forces can be important in the closure region. Here, the Weber number (Eq. 3) is defined using the density of water ρ, a lengthscale $\mathcal{L}$ which was in this case chosen as the depth of the recess, the free-stream velocity $\mathbf{V}$ and the surface tension of water σ. The length scales used for Fr and Re (Eqs. 1 and 2) were based on the recess length. Mäkiharju found that when both $Re > Re_{crit} \approx 1.5 * 10^5$ and $We > We_{crit} \approx 600$, the required air flux is probably a function of Froude number and geometry alone.

$$\mathbf{We} = \frac{\rho \mathcal{L} \mathbf{V}^2}{\sigma} \tag{3}$$

Similar to Zverkhovskyi's findings for the external cavity flows, the above mentioned groups point out the re-entrant jet as well as wave pinch-off as the two possible mechanisms for air discharge from the internal cavity closure region.

2. ON THE STABILITY OF AIR LAYERS AND CAVITIES

The effectiveness of the air layer- and cavity methods with respect to frictional drag reduction depends on the stability of these air layers. This section identifies the mechanisms that are causing instabilities at the free surface of this parallel two-phase flow. These mechanisms ultimately limit separated flow regimes and cause transition from the separated flow regime (air layers and cavities) to a more disperse/elongated bubble flow regime. Both the re-entrant jet mechanism and the wave pinch-off mechanism are pointed out as the two possible mechanisms for air discharge at the cavity closure. Here, it is provisionally assumed that the re-entrant jet and wave pinch-off mechanisms are similar for both the internal and external cavity cases.

This part on the stability of air layers and cavities will focus on the wave pinch-off mechanism. The main question asked in this section is where the small waves come from which are believed to be responsible for the shedding of air from the cavity. The physical mechanism which is believed to be responsible for the re-entrant jet is discussed in section 3.1 of this article.

An example of the waves on a cavity surface is shown in Figure 4. Zverkhovskyi distinguishes two types of waves on the free surface [2]. The first type (Figure 4A) is believed to be caused by turbulent fluctuations in the water at the interface. Their wavelengths are in the order of 0.5-2 cm. These waves are also called capillary-gravity waves. In this regime, the wavelengths are too small to neglect surface tension effects on the waves and too large to neglect the effects from gravity. A detailed discussion on these waves can be found in the work of Brocchini and Peregrine [15]. Similar waves are observed in Figure 3. Free-surface waves with

wavelengths of the same order of magnitude are also observed in the publications of Mäkiharju [14]. In the next section, the main mechanism behind the formation of these capillary-gravity waves at the free surface of the cavity is explained. The second wave type as shown in Figure 4B is characterised by the diverging waves and their reflections from the side walls. These waves are generated by the transverse discontinuities in the flow, occurring at the edges and corners of the cavity.

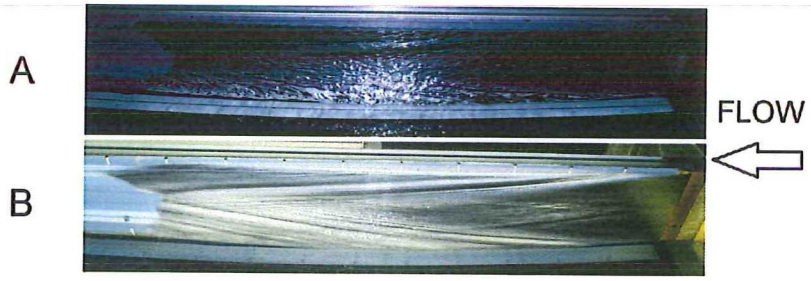

Figure 4 – Different wavesystems on the external cavity surface, V=1.5 m/s. A: instantaneous wave profile. B: time averaged wave profile (reproduced from [2]).

2.1 Stability theory for parallel two-phase flow

Brennen [16] states that separated flow regimes such as stratified horizontal flow can become unstable when waves are formed on the interface. In case these waves continue to grow in amplitude, a transition to another flow regime can occur. These so-called Kelvin-Helmholtz instabilities are one of the most well-known instabilities in parallel two-phase flow. Brennen describes this class of instabilities as the interplay of at least two of the following three types of forces:

- The buoyancy force due to gravity. This force is proportional to $\mathbf{g}\ell^3\Delta\rho$, where ℓ is a typical dimension of the waves and $\Delta\rho$ is the difference in density between the two fluids.
- The surface tension force, characterised by $\sigma\ell$
- A pressure acting on the interface due to a velocity gradient resulting from the displacement of the interface. This is characterised by $\rho(\Delta\mathbf{u})^2\ell^2$, where $\Delta\mathbf{u}$ is the velocity difference between the two fluids.

The buoyancy and surface tension forces are believed to have a stabilising effect in the case of air cavities. When the overlying fluid is less dense than the underlying fluid, such as for air layer and air cavity flows, the component of gravity in the normal direction of the interface stabilises the interface after a small perturbation. The latter of the three force types however is ascribed to a velocity-induced pressure difference and is in all cases destabilising. It is noted that this analysis assumed infinitely thick fluid layers, thus the influence of the cavity thickness and shallow water effect are not taken into account in this analysis yet.

This analysis also negnects viscous effects. However, for the flow regimes of interest in the current study this assumption can not be made. The origin of the small capillary-gravity waves most probably lies in the turbulence intensity in the liquid near the interface (see section 1.2.2 and Figure 3). The destabilising turbulence structures primarily develop in the boundary layer upstream of the cavity.

2.2 Destabilising forces

Boomkamp and Miesen [17] have also made a classification of instabilities in parallel two-phase flows. Their classification is based on linear theory and the rate of change of kinetic energy of the disturbances causing the particular instability. They describe a destabilising Reynolds stress originating from the fluid with the lowest kinematic viscosity. It is stated that when the Reynolds number is large, the destabilising Reynolds stress is primarily produced due to the no-slip conditions at the wall. The Reynolds stress term is often interpreted as the term in the total stress tensor in the fluid which accounts for the turbulent fluctuations in fluid momentum. Zverkhovskyi [2] already pointed out that the waves at the air-water interface were probably caused by turbulent fluctuations. The perturbations are more pronounced when the boundary layer thickness and thus turbulence intensity and length scale increase (Figure 3).

3. GOVERNING PHYSICS IN THE CLOSURE REGION

This section explains both the re-entrant jet mechanism and the wave pinch-off mechanism. These mechanisms are believed to govern the shedding of air pockets from both internal and external cavities.

3.1 Re-entrant jet mechanism

The re-entrant jet mechanism is hold responsible for the break-up of natural sheet cavities into cloud cavities. Callenaere et al. [18] describe the mechanism as follows. In the closure regions of sheet cavities, a region with high adverse pressure gradient is formed. This increase in local pressure forces a thin stream of liquid into the cavity. This thin stream is called the re-entrant jet. Impingement of this jet with the gas-liquid interface results in a disturbance leading to a portion of the attached cavity to be pinched off and advected with the flow. For the present, it is assumed that the re-entrant jet mechanism as observed for natural sheet cavity flows is similar for the ventilated cavity flows of interest in this study.

3.2 Wave pinch-off mechanism

The wave pinch-off mechanism is hypothesised to be governed by the capillary-gravity waves at the air-water interface. When their wave amplitude equals the cavity thickness, these waves 'pinch-off' parts of the cavity. The main stresses responsible for the formation of these waves are possibly the destabilising Reynolds stresses as explained in section 2.2. The stabilising forces at the interface are the surface tension force and the buoyancy force. Questions to be asked are to what extent the stabilising forces are sufficient, whether there is any scale effect on e.g. the surface tension force and what the length scales of the turbulence structures causing these Reynolds stresses are. Are these scales in the order of the boundary layer thickness or the order of the wave amplitude?

4. NUMERICAL MODELLING

The main goal of this current research project is to gain the required knowledge and understanding to model and accurately predict the effect of air lubrication systems on the ship's resistance using CFD. From a practical point of view, this means that only Reynolds-averaged Navier-Stokes (RaNS) methods are of interest. More demanding models such as Large Eddy Simulation (LES) are not believed to be viable for practical ship design purposes yet, due to

the significant amount of added computational time. These scale resolving models can however be used to identify the physical conditions in the closure region and to study and identify scaling influences. Thereafter, one could for example complement RaNS models with dispersion models. The dispersion (or diffusion) of the gas phase is then modelled by an extra convection-diffusion term. This extra term can for example be activated when the conditions characterised by the physics in the closure region are met.

4.1 CFD solver

The preliminary solver to be used for the remaining work is ReFRESCO [19]. It is a viscous-flow CFD code that solves multiphase (unsteady) incompressible flows using the RaNS equations. It is complemented with turbulence models, cavitation models and volume-fraction transport equations for different phases. The equations are discretised using a finite-volume approach. Time integration is performed implicitly with first- or second-order backward schemes. The implementation is face-based, which permits grids with elements consisting of an arbitrary number of faces (hexahedrals, tetrahedrals, prisms, pyramids, etc.) and if needed h-refinement (hanging nodes). For turbulence modelling, RaNS/URaNS, SAS (Scale Adaptive Simulation) and DES (Detached Eddy Simulation) approaches can be used and PANS (Partially-averaged Navier-Stokes) and LES are currently being studied.

4.2 Numerical modelling of the re-entrant jet mechanism

RaNS methods can be used to simulate unsteady natural sheet cavity dynamics and in particular the re-entrant jet mechanism. It is therefore believed that these models are also able to model the re-entrant jet mechanism in case of the ventilated cavity flows of interest for this study. However, the commonly used two-equation turbulence models, such as the k-ε and k-ω models, were originally developed for RANS simulation of single-phase flows. A frequently encountered problem with these turbulence models based on the Boussinesq assumption is the over-prediction of the eddy-viscosity in and downstream of the cavity closure region [20]. Li et al.[20] suspect that the unsteadiness of sheet cavitation is significantly dampened by the viscosity. According to Reboud [21], this over-predicted eddy-viscosity reduces the development of the re-entrant jet and can thus prevent the occurrence of shedding. The above-mentioned tendency is not just associated with one specific RaNS solver or cavitation model. Several additional correction models exist to artificially lower the over-predicted eddy-viscosity, of which the Reboud-correction is one. In these cases a modification the the formulation for the turbulence viscosity is applied. The originally computed turbulence viscosity μ_t is multiplied by a function of the local density $\mathbf{f}(\rho)$ [21].

4.3 Numerical modelling of the wave pinch-off mechanism

RaNS turbulence models only model the effect of turbulence on the general flow. However, when the wave pinch-off mechanism is governed by turbulence structures in the flow, more turbulence scales in the flow have to be resolved to identify the scale of these structures. Scale Resolving Simulation (SRS) models could e.g. help to resolve the larger scales of turbulence in the flow. SRS models have been developed to fulfil the gap between RaNS and LES models. LES models are significantly more demanding in terms of CPU requirements when compared to RaNS models, in particular for wall-bounded flows. Most of the SRS turbulence models use RaNS models in the boundary layers, whereas LES or LES-based models are used in detached regions. SAS, DES, and XLES (eXtra Large Eddy Simulation) are examples of such modelling

approaches. The computational demands are substantially reduced with respect to full LES models, but still much larger than for RaNS models [22]. These models are also available in ReFRESCO, and further research will be carried out using these hybrid models as well as pure LES.

CONCLUSIONS AND FURTHER WORK

Two main mechanisms responsible for air losses in the cavity closure region are identified: the re-entrant jet and wave pinch-off mechanisms. The re-entrant jet mechanism can be modelled using RaNS/VOF methods since there are believed to be large similarities to the natural sheet cavitation shedding mechanism. An eddy-viscosity correction model can be applied in case the eddy-viscosity is over-predicted in the closure region, preventing the development of the re-entrant jet. Further research can be carried out on the sensitivity of this re-entrant jet mechanism to the geometry of the computational domain and eddy-viscosity models.

The capillary-gravity waves that are hold responsible for the wave pinch-off mechanism are hypothesised to be formed due to the large Reynolds stresses in the flow. The involved turbulence structures are generated at the wall upstream of the cavity and destabilise the free surface, resulting in waves with wavelengths in the order of 0.5-2cm. The stabilising forces at the interface are the surface tension force and the buoyancy force. Questions remaining for future research are to what extent the stabilising forces are sufficient, whether there is any scale effect on e.g. the surface tension force and what the length scales of the turbulent structures causing these Reynolds stresses are. These questions are to be answered using Scale Resolving Simulations (SRS) methods. When there is a better understanding of the physics involved in the closure region, an engineering model can e.g. be developed in order to also model the air cavities with a RaNS/VOF method, which can be used for practical ship design purposes.

ACKNOWLEDGEMENTS

This research is financially supported by the Dutch Technology Foundation STW (grant #13265), which is part of the Netherlands Organisation for Scientific Research (NWO), and which is partly funded by the Ministry of Economic Affairs.

REFERENCES

1. Gorbachev, Y. and Amromin, E. (2012) "Ship Drag Reduction by Hull Ventilation from Laval to Near Future: Challenges and Successes", *ATMA 2012*

2. Zverkhovskyi, O. (2014) "Ship Drag Reduction by Air Cavities", *Ph.D. Thesis*, TU Delft

3. Zverkhovskyi, O., Kerkvliet, M., Vaz, G. and van Terwisga, T. (2015) "Numerical Study on Air Cavity Flows", *NuTTS '15*, Cortona, Italy

4. Shiri, A., Leer-Andersen, M.,Bensow, R.E. and Norrby, J. (2012) "Hydrodynamics of a Displacement Air Cavity Ship" *29th Symposium on Naval Hydrodynamics*, Gothenburg, Sweden

5. Murai, Y. (2014) "Frictional drag reduction by bubble injection" *Exp. Fluids* 55:1773

6. Sanders, W.C., Winkel, E.S., Dowling, D.R., Perlin, M. and Ceccio, S.L. (2006) "Bubble friction drag reduction in a high-Reynolds-number flat-plate turbulent boundary layer" *J. Fluid Mech.* 552,353-380

7. Harleman, M.J.W. (2012) "On the effect of turbulence on bubbles: experiments and numerical simulations of bubbles in wall-bounded flows" *Ph.D. Thesis*, TU Delft, The Netherlands

8. Van den Berg, T., Van Gils, D., Lathrop, D. and Lohse, D. (2007) "Bubbly Turbulent Drag Reduction is a Boundary Layer Effect" *Phys. Rev. Lett.* 98:084501

9. Ceccio, S.L. (2010) "Friction Drag Reduction of External Flows with Bubble and Gas Injection" *Annu. Rev. Fluid Mech.* 42,183-203

10. Elbing, B.R., Mäkiharju, S.A., Wiggins, A., Perlin, M., Dowling, D.A. and Ceccio, S.L. (2013) "On the scaling of air layer drag reduction" *J. Fluid Mech.* 717,484-513

11. Fukuda, K., Tokunaga, J., Nobunaga, T., Nakatani, T., Iwasaki, T. and Kunitake, Y. (2000) "Frictional drag reduction with air lubricant over a super-water- repellent surface" *J. Mar Sci Technol* 5:123-130

12. Butuzov, A.A. (1966) "Limiting Parameters of an Artificial Cavity Formed on the Lower Surface of a Horizontal Wall" *Izv. AN SSSR. MZhG [Fluid Dynamics]* Vol 1: No.2: 167-170

13. Matveev, K.I. (2003) "On the limiting parameters of artificial cavitation" *Ocean Engineering* 30:1179-1190

14. Mäkiharju, S.A. (2012) "The Dynamics of Ventilated Partial Cavities over a Wide Range of Reynolds Numbers ans Quantitative 2D X-Ray Densitometry for Multiphase Flow" *Ph.D. Thesis* The University of Michigan

15. Brocchini, M. and Peregrine, D.H. (2001) "The dynamics of strong turbulence at free surfaces. Part 1. Description" *J. Fluid Mech.* 449, 225–254

16. Brennen, C.E. (2005) "Fundamentals of Multiphase Flow" *Cambridge University Press*, Cambridge

17. Boomkamp, P.A.M. and Miesen, R.H.M. (1996) "Classification of instabilities in parallel two-phase flow", *Int. J. Multiphase Flow* 22, 67-88

18. Callenaere, M., Franc, J.-P., Michel, J.-M. and Riondet, M. (2001) "The cavitation instability induced by the development of a re-entrant jet". *J. Fluid Mech* 444, 223-256

19. ReFRESCO (2016) `http://www.marin.nl/refresco`, Online; accessed 25 April 2016

20. Li, D., Grekula, M. and Lindell, P. (2009) "A modified SST k-ω Turbulence Model to Predict the Steady and Unsteady Sheet Cavitation on 2D and 3D Hydrofoils", *Proceedings of the 7th International Symposium on Cavitation CAV2009*, Ann Arbor, Michigan, USA

21. Reboud, J., Stutz, B. and Coutier, O. (1998) "Two-phase Flow Structure of Cavitation: Experiment and modelling of Unsteady Effects", *Third International Symposium on Cavitation*, Grenoble, France

22. Pereira, F., Vaz, G. and Eça, L. (2015) "On the Numerical Requirements of RaNS and Hybrid Turbulence Models", *VI International Conference on Computational Methods in Marine Engineering*, Rome, Italy